Published in final edited form as:

Science. 2017 May 19; 356(6339): 757–759. doi:10.1126/science.aah6895.

A placental growth factor is silenced in mouse embryos by the zinc finger protein ZFP568

Peng Yang[1], **Yixuan Wang**[1,2], **Don Hoang**[1], **Matthew Tinkham**[1], **Anamika Patel**[3], **Ming-An Sun**[1], **Gernot Wolf**[1], **Mairead Baker**[1], **Huan-Chieh Chien**[4,5], **Kuan-Yu Nick Lai**[4,5], **Xiaodong Cheng**[3], **Che-Kun James Shen**[4,5,*], and **Todd S. Macfarlan**[1,*]

[1]The Eunice Kennedy Shriver National Institute of Child Health and Human Development, National Institutes of Health, Bethesda, MD 20892, USA.

[2]Clinical and Translational Research Center of Shanghai First Maternity and Infant Hospital, School of Life Sciences and Technology, Tongji University, Shanghai 200092, China.

[3]Department of Biochemistry, Emory University School of Medicine, Atlanta, GA 30322, USA.

[4]Department of Life Sciences and Institute of Genome Sciences, National Yang-Ming University, Taipei, Taiwan, Republic of China.

[5]Institute of Molecular Biology, Academia Sinica, Taipei, Taiwan, Republic of China

Abstract

Insulin-like growth factor 2 (IGF2) is the major fetal growth hormone in mammals. We identify zinc finger protein 568 (ZFP568), a member of the rapidly evolving Kruppel-associated box-zinc finger protein (KRAB-ZFP) family linked primarily to silencing of endogenous retroelements, as a direct repressor of a placental-specific *Igf2* transcript (designated *Igf2-P0*) in mice. Loss of *Zfp568*, which causes gastrulation failure, or mutation of the ZFP568-binding site at the *Igf2-P0* promoter causes inappropriate *Igf2-P0* activation. Deletion of *Igf2* can completely rescue *Zfp568* gastrulation phenotypes through late gestation. Our data highlight the exquisite selectivity with which members of the KRAB-ZFP family repress their targets and identify an additional layer of transcriptional control of a key growth factor regulating fetal and placental development.

Insulin-like growth factor 2 (IGF2) plays a key role in regulating fetoplacental development. Deletion of *Igf2* or its receptor *Igf1r* leads to placental and fetal growth restriction in mice (1,2), and misregulation of IGF2 in humans causes the undergrowth and overgrowth conditions Russell-Silver syndrome (3) and Beckwith-Wiedemann syndrome (4), respectively. In mice, *Igf2* is maternally imprinted and is differentially regulated in the placenta and fetus. It is transcribed from three promoters (designated *Igf2-P1, P2,* and *P3*) in both the fetus and placenta and additionally from a fourth placental-specific promoter designated *Igf2-P0*. The placental *Igf2-P0* transcript is expressed in the labyrinth trophoblast

*Corresponding author. todd.macfarlan@nih.gov (T.S.M.); ckshen@gate.sinica.edu.tw (C.-K.J.S.).

SUPPLEMENTARY MATERIALS

www.sciencemag.org/content/356/6339/757/suppl/DC1

and accounts for ~10% of the total placental expression of *Igf2* (5). Mice lacking paternal *Igf2-P0* display intrauterine growth restriction, reduced growth of the placenta (6, 7), and increased reactivity to anxietypromoting stimuli as a result of the mismatch between placental supply and fetal demand for nutrients (8). However, *Igf2* is expressed at low levels in preimplantation development and in embryonic stem cells (ESCs), suggesting an important requirement for *Igf2* repressors at implantation. Here we identify ZFP568, a Kruppel-associated box-zinc finger protein (KRAB-ZFP), as the direct repressor of *Igf2-P0* in early development.

ZFP568 is an essential factor that regulates convergent extension during gastrulation (9–11). To determine genes that may be regulated by ZFP568, we crossed mice harboring a floxed *Zfp568* allele fused to a C-terminal green fluorescent protein (GFP) tag (*Zfp568-GFP*$^{FL/FL}$) (fig. S1A) with Rosa26-CreERT2 mice and derived ESC and trophoblast stem cell (TSC) lines from blastocysts (fig. S1B) (12). Treatment of cells with 4-hydroxytamoxifen (4-OHT), which activates the CreERT recombinase, resulted in deletion of *Zfp568* and loss of ZFP568-GFP protein (fig. S1, C and D). Only two genes were significantly affected by acute *Zfp568* deletion in ESCs and TSCs: *Zfp568* itself and *Igf2-P0*, which was activated an average of eightfold (Fig. 1A; figs. S1E and S2, A and B; and table S1). Clustering analysis confirmed that differences between independently derived cell lines were greater than differences observed before and after *Zfp568* deletion (fig. S2C). Furthermore, there was no misregulation of repetitive elements (fig. S2D). RNA-sequencing (RNA-seq) and quantitative reverse transcription polymerase chain reaction (qRT-PCR) confirmed that only the placental-specific *Igf2-P0* promoter and transcript were activated, whereas the fetal promoters and the *Igf2* antisense (*Igf2as*) transcripts were not affected (fig. S2, A, B, E, and F). The increased expression of *Igf2-P0* also significantly increased the IGF2 peptide levels secreted in the media in ESCs. There was no significant increase in IGF2 peptide upon *Zfp568* deletion in TSCs (fig. S2G), which express high levels of *Igf2-P1, P2,* and *P3* transcripts even in wild-type (WT) cells (fig. S2, B and F).

To determine whether *Zfp568* deletion leads to allelic activation of *Igf2*, we used clustered regularly interspaced short palindromic repeats (CRISPR)-Cas9 engineering to delete *Zfp568* in CAST/Eij; C57BL/6 hybrid ESCs (fig. S3, A and B), which contain single-nucleotide polymorphisms (SNPs) that allow discrimination of parental *Igf2* alleles. Consistent with results from acute deletion of *Zfp568,* chronic deletion of *Zfp568* in hybrid cells resulted in reactivation not only of *Igf2-P0,* but also of *P1, P2,* and *P3* transcripts (fig. S3, C to F), suggesting that the reactivation spread to neighboring promoters over prolonged culture. Most of the *Igf2-P0* transcripts were transcribed from the paternal allele (Fig. 1B and fig. S3G). We also found extensive dysregulation of additional genes in hybrid *Zfp568*$^{KO/KO}$ cells likely caused by chronic loss of *Zfp568* and overexpression of IGF2, as these effects could be partially mimicked by exposing WT hybrid ESCs to IGF2 peptide (fig. S3, E and H).

To determine whether ZFP568 directly represses *Igf2-P0,* we performed chromatin immunoprecipitation sequencing (ChIP-seq) with antibodies against GFP on *Zfp568-GFP*$^{FL/FL}$ ESCs and TSCs. We found 137 and 86 high-confidence ZFP568-binding peaks in ESCs and TSCs, respectively (table S2), which include a peak upstream of the *Igf2-P0*

promoter (Fig. 2A). Motif analysis revealed a highly significant binding motif of 21 to 24 base pairs (bp) in both ESCs and TSCs, with a large fraction of the most highly enriched peaks containing the target motif, including *Igf2-P0* (fig. S4A). The most-enriched 29 peaks were also shared by both ESCs and TSCs (fig. S4A). ZFP568 binding was only weakly correlated with KRAB-associated protein-1 (KAP1) and SET domain bifurcated 1 (SETDB1) binding and was not substantially marked by trimethylated histone H3 lysine 9 (H3K9me3) (fig. S4B). In contrast, the *Igf2-P0* promoter contained a strong H3K9me3 signal that was completely lost upon *Zfp568* deletion (Fig. 2A). Furthermore, deletion of the KRAB-ZFP corepressors *Setdbl* and *Trim28/KAP1* resulted in derepression of *Igf2-P0* and loss of H3K9me3 (fig. S4, C and D). Additionally, there was a corresponding loss of DNA methylation at an *Igf2-P0* CpG island designated DMR0, but not at DMR1 or DMR2, upon loss of *Zfp568* (fig. S5, A to C).

To verify the binding site of ZFP568, we performed luciferase reporter assays using minimal putative ZFP568-binding sites and the full *Igf2-P0* promoter (fig. S6, A and B). Expression of ZFP568 significantly repressed reporters containing the minimal *Igf2-P0* binding site or with the consensus binding site (Fig. 2B). Likewise, ZFP568 repressed the full *Igf2-P0* reporter (fig. S6B). Point mutation of the KRAB domain that mimics the previously described Chato mutation (11) prevented repression of the reporters (fig. S6C). Furthermore, triplet scrambling of the *Igf2-P0* binding site or deletion of pairs of zinc fingers had a significant impact on transcriptional repression (fig. S6, D and E). Because the binding site contains a CpG dinucleotide, we speculated that ZFP568 binding to its target may be methylation sensitive (fig. S6B). However, bisulfite sequencing in ESCs demonstrated that these CpG sites are not methylated (fig. S6F). Furthermore, we expressed in *Escherichia coli* and purified the 11–zinc finger array of ZFP568 and measured its binding affinity to a 26-bp double-stranded oligonucleotide encompassing the *Igf2-P0* binding site using fluorescence polarization (13). We found that the ZFP568 zinc fingers bound specifically to the *Igf2-P0* binding site with a K_d of ~8 nM (Fig. 2C). Methylation of the CpG site caused a modest reduction (about threefold) in binding affinity, whereas methylation of the two CpA sites had a more significant effect, consistent with these positions being more conserved (fig. S6G).

To confirm that ZFP568 was acting through its binding site within the *Igf2-P0* promoter to repress *Igf2-P0,* we used CRISPR/Cas9 to mutate the ZFP568-binding site in *Zfp568-GFP*$^{FL/FL}$ ESCs (Fig. 3A). ESC lines harboring distinct small deletions encompassing the binding site displayed increased expression of *Igf2-P0*, coincident with the loss of ZFP568 binding specifically at the *Igf2-P0* locus (Fig. 3, B and C, and fig. S7, A to C). Treatment of binding site-mutant ESCs with 4-OHT (to delete *Zfp568)* did not further increase the expression of *Igf2-P0* (Fig. 3B), indicating that ZFP568 repression activity is binding site dependent. ChIP-seq and DNA methylation analysis revealed loss of H3K9me3 in ZFP568 binding site-mutant ESCs and loss of DNA methylation at DMR0 (Fig. 3C and fig. S7D). These data demonstrate that ZFP568 maintains a heterochromatin state at the *Igf2-P0* promoter by direct interaction with its binding site.

Consistent with our ESC and TSC data, we also found *Igf2-P0* levels to be increased in *Zfp568*$^{KO/KO}$ embryos (Fig. 4A and fig. S8, A to D), which fail to complete gastrulation and which display phenotypes similar to the previously described Chato mutants, including

convergent-extension failure and a yolk sac membrane-ruffling phenotype (that could be easily visualized and scored using autofluorescence microscopy) and arrest by embryonic day 9 (E9) (fig. S8, E and F) (9,10). *Zfp568F*$^{KO/KO}$ embryonic tissues also displayed reduced methylation specifically at *Igf2* DMR0 (fig. S8, G and H). We thus reasoned that overexpression of IGF2 may contribute to the early embryonic lethality of *Zfp568* mutants. To test this idea, we crossed *Zfp568* knockout (KO) mice with *Igf2* KO mice (14) (containing a deletion in the final exon, thus disrupting all *Igf2* transcript variants) to determine if deletion of *Igf2* could rescue the lethal phenotype. Loss of paternal *Igf2* expression was sufficient to completely restore viability of *Zfp568*$^{KO/KO}$ embryos through mid-gestation, as *Zfp568*$^{KO/KO}$*; Igf2*$^{pat/+}$ embryos and fetuses were found at near Mendelian ratios and indistinguishable from *Zfp568* WT littermates at E12.5 to 18.5 (Fig. 4B and fig. S9A). Despite this lack of gross morphological phenotype at late fetal stages, only two *Zfp568*$^{KO/KO}$*; Igf2*$^{KO/KO}$ pups have been recovered after birth, both of which were found dead (fig. S9, B and C). Nonetheless, these data demonstrate a genetic interaction between *Zfp568* and *Igf2*.

Our results provide biochemical and genetic evidence that the KRAB-zinc finger protein ZFP568 is a specific and direct repressor of *Igf2-P0* in mice. Recent studies have revealed that the majority of KRAB-ZFPs interact with and likely restrict the expression of specific retrotransposon families, potentially facilitating the domestication of retrotransposons and the evolution of gene regulatory networks (15–19). Whether the binding site for ZFP568 at *Igf2-P0* was derived from an ancient and since decayed retrotransposon or was generated by genetic drift is unknown, but our findings nonetheless demonstrate that KRAB-ZFPs can evolve essential roles in precision developmental gene silencing. Notably, ZFP568 orthologs have been detected in all eutherian mammals examined and contain a conserved zinc “fingerprint” (16), suggesting that their DNA-binding specificity is conserved. Intriguingly, *Zfp57*, another KRAB-ZFP that emerged in mammals, is a critical factor that maintains genomic imprints at *Igf2-P0* (20,21), a process linked to viviparity (22).

Furthermore, the human *Zfp568* ortholog, *Znf568*, is among the most-rapidly evolving human genes, with three common allele variants found within human populations that have been linked to relative head size at birth (12). Thus, KRAB-ZFP/KAP1-dependent regulation of *Igf2-P0* has shaped, and likely continues to shape, the evolution of mammals.

Supplementary Material

Refer to Web version on PubMed Central for supplementary material.

ACKNOWLEDGMENTS

We thank K. Pfeifer and C. Gebert for *Igf2* KO mice. We thank S. Coon, J. Iben, and T. Li for Next Generation Sequencing (NGS) support. This work was supported by NIH grants 1ZIAHD008933 (T.S.M.) and GM049245-23 (A.P. and X.C.), Ministry of Science and Technology (MOST) Frontier of Science Award, Academia Sinica Senior Investigator Award (C.-K.J.S.), National Natural Science Foundation of China (NSFC) 31471392, and Future Scientists Exchange Program of the China Scholarship Council (CSC) (Y.W.). NGS data have been deposited in the Gene Expression Omnibus (GEO) database (GSE84832). *Zfp568-GFP*$^{FL/FL}$ mice are available from C.-K.J.S. under a material transfer agreement with the Academia Sinica, Taipei, Taiwan, Republic of China.

REFERENCES AND NOTES

1. Baker J, Liu JP, Robertson EJ, Efstratiadis A, Cell 75, 73–82 (1993). [PubMed: 8402902]
2. Liu JP, Baker J, Perkins AS, Robertson EJ, Efstratiadis A, Cell 75, 59–72 (1993). [PubMed: 8402901]
3. Gicquel C et al., Nat. Genet 37, 1003–1007 (2005). [PubMed: 16086014]
4. Weksberg R, Shuman C, Smith AC, Am. J. Med. Genet 137C, 12–23 (2005). [PubMed: 16010676]
5. Moore T et al., Proc. Natl. Acad. Sci. U.S.A 94, 12509–12514 (1997). [PubMed: 9356480]
6. Constância M et al., Nat. Genet 26, 203–206 (2000). [PubMed: 11017078]
7. Constância M et al., Nature 417, 945–948 (2002). [PubMed: 12087403]
8. Mikaelsson MA, Constância M, Dent CL, Wilkinson LS, Humby T, Nat. Commun 4, 2311 (2013). [PubMed: 23921428]
9. García-García MJ, Shibata M, Anderson KV, Development 135, 3053–3062 (2008). [PubMed: 18701545]
10. Shibata M, García-García MJ, Dev. Biol 349, 331–341 (2011). [PubMed: 21094155]
11. Shibata M, Blauvelt KE, Liem KF, Jr., García-García MJ, Development 138, 5333–5343 (2011). [PubMed: 22110054]
12. Chien HC et al., PLOS ONE 7, e47481 (2012). [PubMed: 23071813]
13. Patel A, Horton JR, Wilson GG, Zhang X, Cheng X, Genes Dev. 30, 257–265 (2016). [PubMed: 26833727]
14. DeChiara TM, Efstratiadis A, Robertson EJ, Nature 345, 78–80 (1990). [PubMed: 2330056]
15. Schmitges FW et al., Genome Res. 26, 1742–1752 (2016). [PubMed: 27852650]
16. Imbeault M, Helleboid P, Trono D, Nature 543, 550–554 (2017). [PubMed: 28273063]
17. Wolf G et al., Genes Dev. 29, 538–554 (2015). [PubMed: 25737282]
18. Ecco G et al., Dev. Cell 36, 611–623 (2016). [PubMed: 27003935]
19. Jacobs FM et al., Nature 516, 242–245 (2014). [PubMed: 25274305]
20. Li X et al., Dev. Cell 15, 547–557 (2008). [PubMed: 18854139]
21. Quenneville S et al., Mol. Cell 44, 361–372 (2011). [PubMed: 22055183]
22. Renfree MB, Suzuki S, Kaneko-Ishino T, Philos. Trans. R. Soc. London B Biol. Sci 368, 20120151 (2013). [PubMed: 23166401]

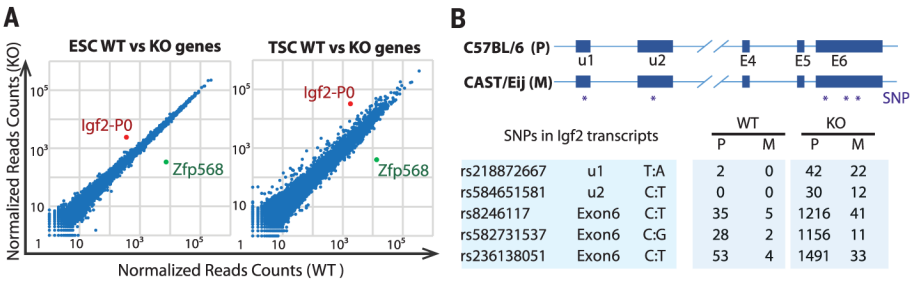

Fig. 1. Acute *Zfp568* knockout leads to derepression of *Igf2-P0*.

(**A**) Scatter plots of gene expression in *Zfp568* WTand KO ESCs and TSCs, as determined by RNA-seq. (**B**) Schematic of SNPs in CAST/Eij; C57BL/6 hybrid ESCs used to discriminate *Igf2* parental alleles. SNP counts from RNA-seq in *Zfp568* WT and KO CAST/Eij; C57BL/6 hybrid ESCs are indicated.

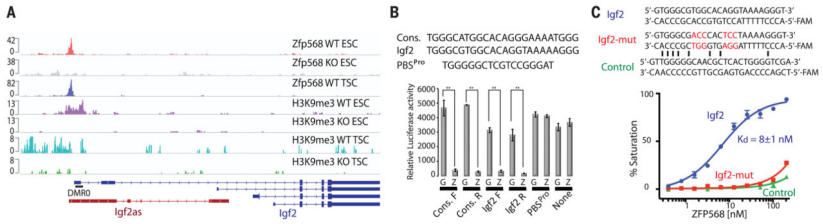

Fig. 2. ZFP568 directly targets *Igf2-P0* for repression.

(**A**) ZFP568 and H3K9me3 ChIP-seq signals at the *Igf2* locus in *Zfp568* WT and KO ESCs and TSCs. DMR0 is a differentially methylated region overlapping exon 1 of the *Igf2-P0* transcript. *Igf2as* is the *Igf2* antisense transcript. (**B**) Relative luciferase activity in 293T cells overexpressing GFP (G) or ZFP568 (Z) and an SV40 promoter–driven luciferase plasmid containing the ZFP568 consensus (cons) or *Igf2* binding site in the forward (F) or reverse (R) orientation. PBS^{Pro} is the 18-nucleotide (nt) primer binding site for proline, which is bound by ZFP809 but not ZFP568. *t* test: Error bars indicate standard deviation; **P < 0.01; $n = 3$. (**C**) Fluorescence-polarization binding assay of ZFP568 (ZnF1-11) protein incubated with indicated 6-carboxyfluorescein (FAM)–labeled double-stranded oligonucleotides.

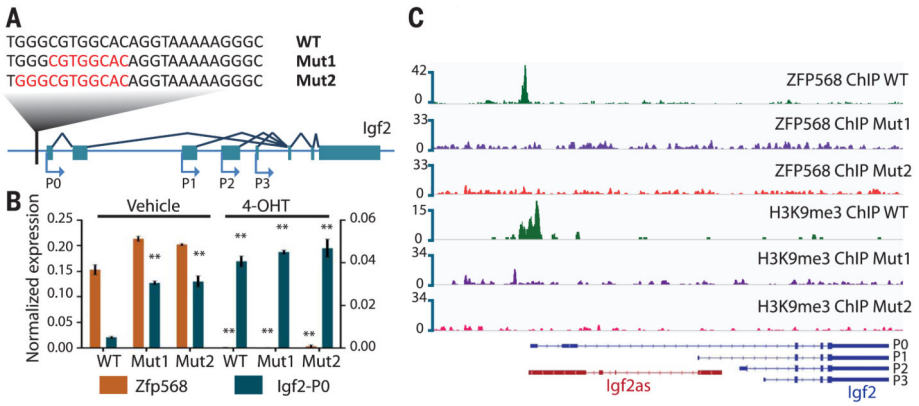

Fig. 3. Mutation of the ZFP568-binding site upstream of the *Igf2-P0* promoter activates *Igf2-P0*.

(**A**) Sequences of WT and two homozygous mutant ESC lines (with deleted nucleotides indicated in red) relative to the consensus binding site for ZFP568. (**B**) *Igf2-P0* and *Zfp568* levels were determined by qRT-PCR in the indicated binding site-mutant ESCs before and after *Zfp568* deletion with 4-OHT. *t* test: Error bars indicate standard deviation; **P < 0.01; *n* = 3. (**C**) ZFP568 and H3K9me3 ChIP-seq signals at *Igf2* in *Zfp568* WT and binding site-mutant ESCs.

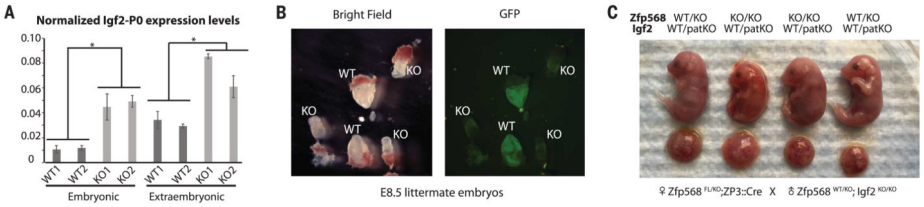

Fig. 4. *Igf2* KO rescues *Zfp568* KO–induced lethality.

(**A**) Relative *Igf2-P0* levels in embryonic and extraembryonic tissues from E8.5 *Zfp568-GFP*$^{FL/FL}$ and *Zfp568*$^{KO/KO}$ littermate embryos. *t* test: Error bars indicate standard deviation; *P < 0.05; $n = 3$. (**B**) Bright-field and GFP-fluorescence images of *Zfp568-GFP*$^{FL/FL}$ and *Zfp568*$^{KO/KO}$ littermate embryos at E8.5. (**C**) Images of pups of indicated genotypes from *Zfp568* KO and paternal (pat) *Igf2* KO crosses at E18.5.